RESULTS

CHAPTER III: RESULTS

The results obtained in the frame of this thesis in the different experiments listed in sections 2.2 and 2.3.

III-1 Consequences of Cyclotron Ion Irradiation :

III-1.1 Visual Inspection of Samples :

The effect of MeV ion irradiation on the physical properties of the organic substances and the minerals were observed for the different sources of radiation. The colour of tetracosane changed from white to slight yellow at low dose and to deep yellow at high dose. After the irradiation of androstane, it had changed from white colour to slight liquid yellow (viscous), naphthalene changed from white to brown colour, gradually with the radiation dose. Anthracene changed from slight yellow to brown colour. There was no change in kerogen colour. It remained black. No change of mineral colour was observed as a consequence of irradiation.

III-1.2 Fourier Transform Infrared Spectroscopy in Transmission:

The changes induced in the materials after the irradiation by H^+, $^3He^{2+}$ and $^4He^{2+}$ ions were monitored by infrared spectroscopy. The integrated absorption coefficient of a given spectral feature can be evaluated from the spectrum.

III-1.2.1 Pure Organic Substances :

Figure 19 compares the infrared spectra in transmission of tetracosane at a maximum dose of H^+ and $^3He^{2+}$ irradiation of 6.1 and 16.4 eV/C atom, respectively, with that of unirradiated sample from wavenumber 4000 to 400 cm^{-1} (2.5 – 25μm wavelength). It can be seen that many new bands appear and some old bands disappear. This means that the tetracosane is much affected by the irradiation. More details are seen in Fig. 20 which shows a detailed representation of the FTIR spectra. It seems that a new band appears at 1470 cm^{-1} (6.8 μm) due to

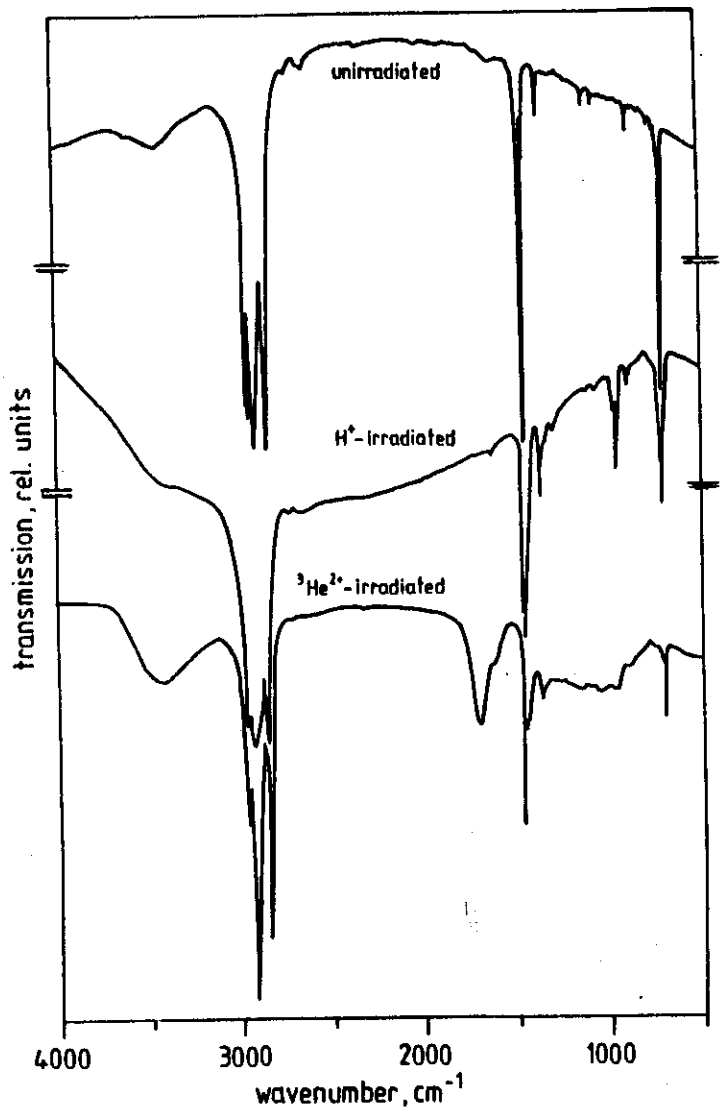

Fig. 19 : Comparison of FT-IR spectrum of tetracosane in transmission at a maximum dose of H^+ and $^3He^{2+}$ ions (6.1 and 16.4 eV per carbon atom, resp.) with that of unirradiated sample.

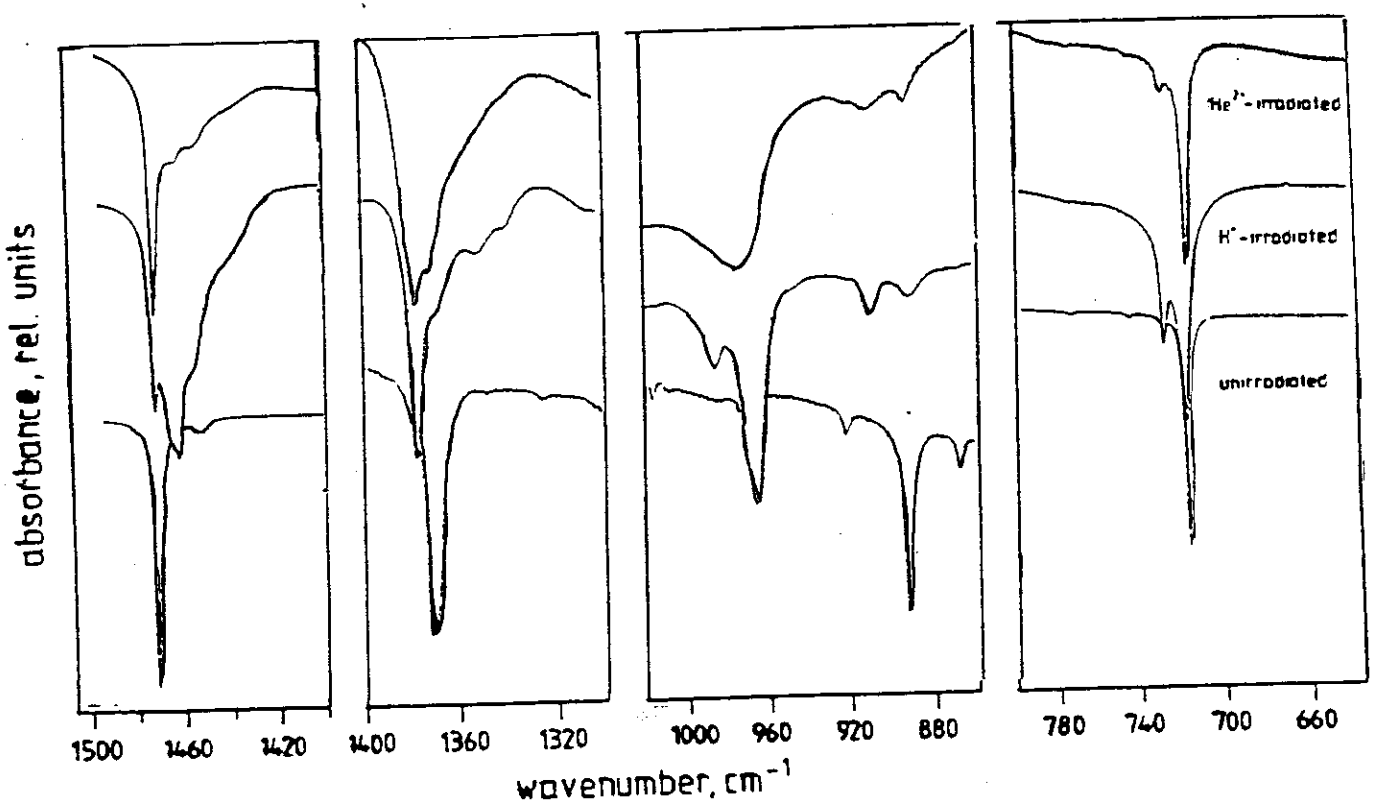

Fig. 20 : Details of the FT-IR spectrum of tetracosane in transmission at a maximum dose of H^+ and $^3He^{2+}$ ions compared with that of unirradiated sample.

$\delta_b(-CH_2-)$ and $\delta_{as}(-CH_3)$ **[64]**. At the same time an old band at 1472 cm^{-1} (6.79 μm) decreases. A 1378 cm^{-1} feature due to $\delta_s(-CH_3)$ shows up accompanied by a decrease of the old feature at 1370 cm^{-1} (7.3 μm). In the region from 1352-1341 cm^{-1} (7.4-7.5 μm) two new very weak bands due to $\delta_s(-CH_3)$ in $-\underset{1}{C}=\overset{1}{C}-CH_3$ were found only in the case of H^+ irradiation. For $^3He^{2+}$ irradiation a feature at 1174 cm^{-1} (8.5 μm) appears, probably due to $C-(CH_3)_2$. Features at 969 and 966 cm^{-1} (10.3 and 10.35 μm) for H^+ and $^3He^{2+}$ irradiation, respectively, are due to δ_{op} (–C–H) in –CH=CH– trans. For H^+ irradiation a feature appears at 987 cm^{-1} (10.13 μm) due to δ_{op} (C–H) in $-CH=CH_2$. For H^+ and $^3He^{2+}$ ion irradiation a new feature appears at 910 cm^{-1} (10.99 μm) due to δ_{op} ($=CH_2$) in $-CH=CH_2$. The old band at 893 cm^{-1} disappears to some extent. The new bands which appear at 730 cm^{-1} (13.7 μm) for H^+ irradiation and at 729 cm^{-1} (13.72 μm) for $^3He^{2+}$ irradiation are due to skeleton vibration. Some decrease occurs for an old band at 718 cm^{-1} (13.93 μm).

Table 9 defines the positions of the old and new bands in tetracosane with the vibration mode, the relative strength and the FWHM (full width at half maximum). More quantitative analysis is carried out in Table 10. The integrated area of selected peaks (old and new bands) is evaluated for different doses. Table 11 quantitatively shows the ratios of different bonds of the radiation products of tetracosane. In principle one evaluates the bond ratio as the ratio between the number of different groups N(group) of the radiation products. N(group) can be determined from integrated absorbance (cm^{-1}) devided by integrated cross section (per group) $cm^2\ cm^{-1}$ for the same group :

$$N(\text{group}) = \frac{A_{int}(\text{group feature})}{\sigma_{int}(\text{the same group})}, \qquad (25)$$

Table 9 : Wavenumbers of old and new bands after irradiation of tetracosane with assignment of vibration mode, its strength and FWHM.

position cm^{-1}	old or new bands after irradiation	vibrational mode	FWHM cm^{-1}	relative strength*
3420	$^3He^{2+}$	ν (O-H) stretching	280	s
2962	old	ν (C-H) stretching	114	s
2926	old		114	s
2872	old		114	s
2853	old		110	s
1718	$^3He^{2+}$	ν (C = O)	94	s
1630	H^+	ν (C = C)	31	w
1630	$^3He^{2+}$		52	w
1472	old	$\delta_b(-CH_2)$, $\delta_{as}(CH_3)$	4	s
1467	H^+		21	s
1467	$^3He^{2+}$		25	m
1455	old	$\delta_s(CH_3)$	5	m
1378	H^+		8	m
1378	$^3He^{2+}$		10	m
1370	old		7	m
1354	H^+	$\delta_s(CH_3)$ in -CH=CH-CH_3	5	vw
1341	H^+		5	vw
1300	H^+	δ_{ip} (C-H) in -CH=CH_2	4	w
1174	$^3He^{2+}$	skeleton vib. in C-$(CH_3)_2$	32	w
1065	$^3He^{2+}$	δ ip (C-H) in trans -CH=CH-	15	w
987	H^+	δ ip (C-H) in -CH=CH_2	13	w
969	$^3He^{2+}$	δ op (C-H) in trans -CH=CH-	36	m
966	H^+		13	m
910	H^+	δ op (CH_2) in -CH=CH_2	8	m
910	$^3He^{2+}$		23	w
893	old	unidentified	15	m
730	H^+	skeleton vib. ($N_c > 6$)	8	m
729	$^3He^{2+}$		6	w
718	old		3	s

* s = strong, m = medium, w = weak, vw = very weak

Table 10: Integrated area of selected peaks (old and new) of tetracosane at different doses for H^+ and $^3He^{2+}$ Ion irradiation.

ion irradiation	dose eV/Catom	peak position, cm^{-1}								
		1467	1378	1174	966	910	893	790	729	718
H^+	0						0.23			3.34
	1.6		0.18		0.92	0.06	0.18		0.35	3.00
	3.2		0.73		0.92	0.06	0.14		1.05	2.17
	6.1	6.76	1.01		2.13	0.29	0.19		1.27	2.24
$^3He^{2+}$	4.1	3.92	0.86	0.12	0.77	0.14	0.07	0.38		1.13
	8.2	3.47	1.26	0.16	0.73	0.17	0.08	0.21		0.89
	16.4	2.87	2.00	0.20	0.74	0.16		0.16		0.51

Table 11 : Bond ratios of the radiation products of tetracosane at H^+ and $^3He^{2+}$ ion irradiation at maximum dose.

bond ratios		
tetracosane	H^+	$^3He^{2+}$
$\frac{N(-CH_2-)}{N(-CH_3)}$	3.0	2.2
$\frac{N(-\overset{1}{C}=\underset{1}{C}-)}{N(-\overset{1}{C}=CH_2)}$	3.5	2.6
$\frac{N(C-C)}{N(C=C)}$	38.5	53

where

A_{int} = integrated absorbance (cm^{-1})

σ_{int} = integrated cross section per group ($cm^2\ cm^{-1}$). The integrated cross sections were taken from Wexler [65].

Fig. 21 shows the spectra of irradiated androstane, a kind of a cyclic paraffin from 4000 to 400 cm^{-1} at maximum doses of H^+ and $^4He^{2+}$ ion irradiation (5.7 and 38.1 eV /C atom, respectively) with that of the unirradiated sample. It can be seen that some old bands disappear and new bands grow. Fig. 22 shows this on an enlarged scale. An old feature at 2960 cm^{-1} (3.38 μm) due to ν_{as} ($-CH_3$) stretching disappears for $H^+$and $^4He^{2+}$ ion irradiation. A new band shows up at 1635 cm^{-1} (6.12 μm) due to ν(C=C) stretching. The 1448 cm^{-1} (6.91 μm) and 1378 cm^{-1} (7.26 μm) features of androstane increase when the sample is irradiated by H^+ and $^4He^{2+}$ ions. Many new bands in the reagion from 1200-700 cm^{-1} (833-14.29 μm) are due to various ring skeleton modes. A feature at 990 cm^{-1} (10.10 μm) showing up for $H^+$and $^4He^{2+}$ ion irradiation may be due to δ(C–H) in $-CH=CH_2$. A broad band at ~ 980 cm^{-1}(10.20 μm) for both irradiations is due to δ_{op}(C–H) in –CH=CH– or ring vibrations. A new band appears also at 910 cm^{-1} (10.99 μm) and is due to $\delta_{op}(CH_2)$ in $-CH=CH_2$. The new feature at 688 cm^{-1}(14.53 μm) only shows up for H^+ irradiation, another feature at 665 cm^{-1} (15.04 μm) for H^+ irradiation and at 669 cm^{-1} (14.95 μm) for $^4He^{2+}$ irradiation. These three bands are due to δ_{op}(C–H) in CH=CH–, inside the ring. Table 12 lists the wavenumber of the old and new bands in androstane with an assignment of the vibration mode and its strength and FWHM. The integrated area of selected peaks (old and new bands) is evaluated for different doses, as shown in Table 13. The bond ratios of the radiation products of the androstane are shown in Table 14.

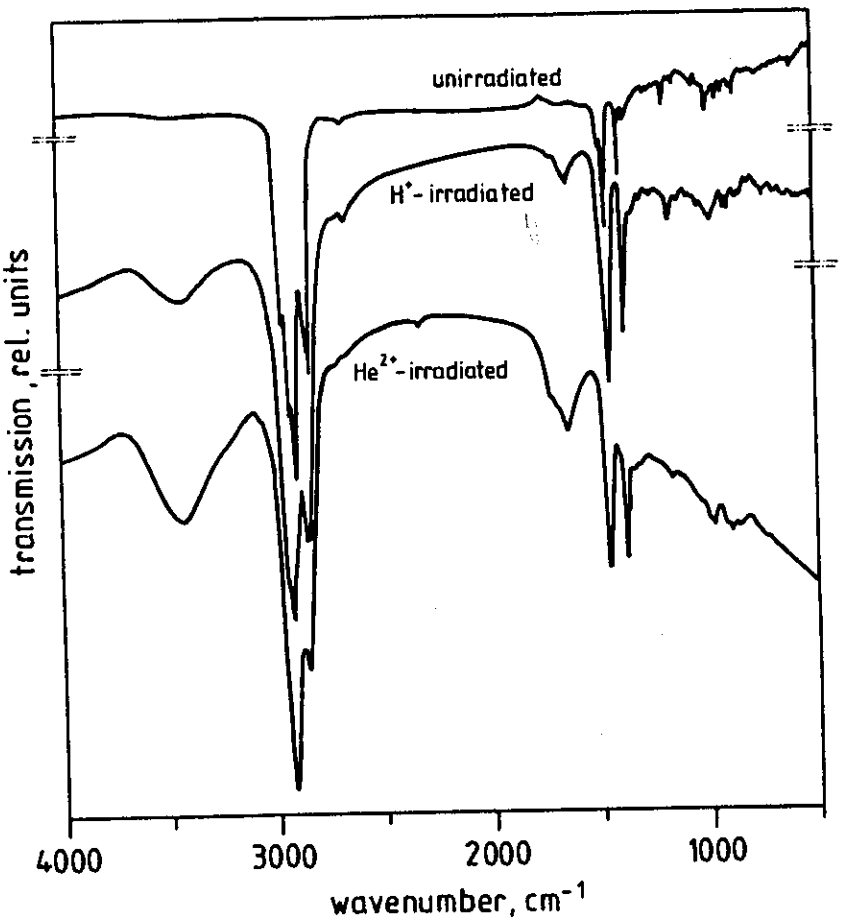

Fig. 21 : Comparison of FT-IR spectrum of androstane in transmission at a maximum dose of H^{+} and $^{4}He^{2+}$ ions (5.7 and 38.2 eV per carbon atom, resp.) with that of unirradiated sample.

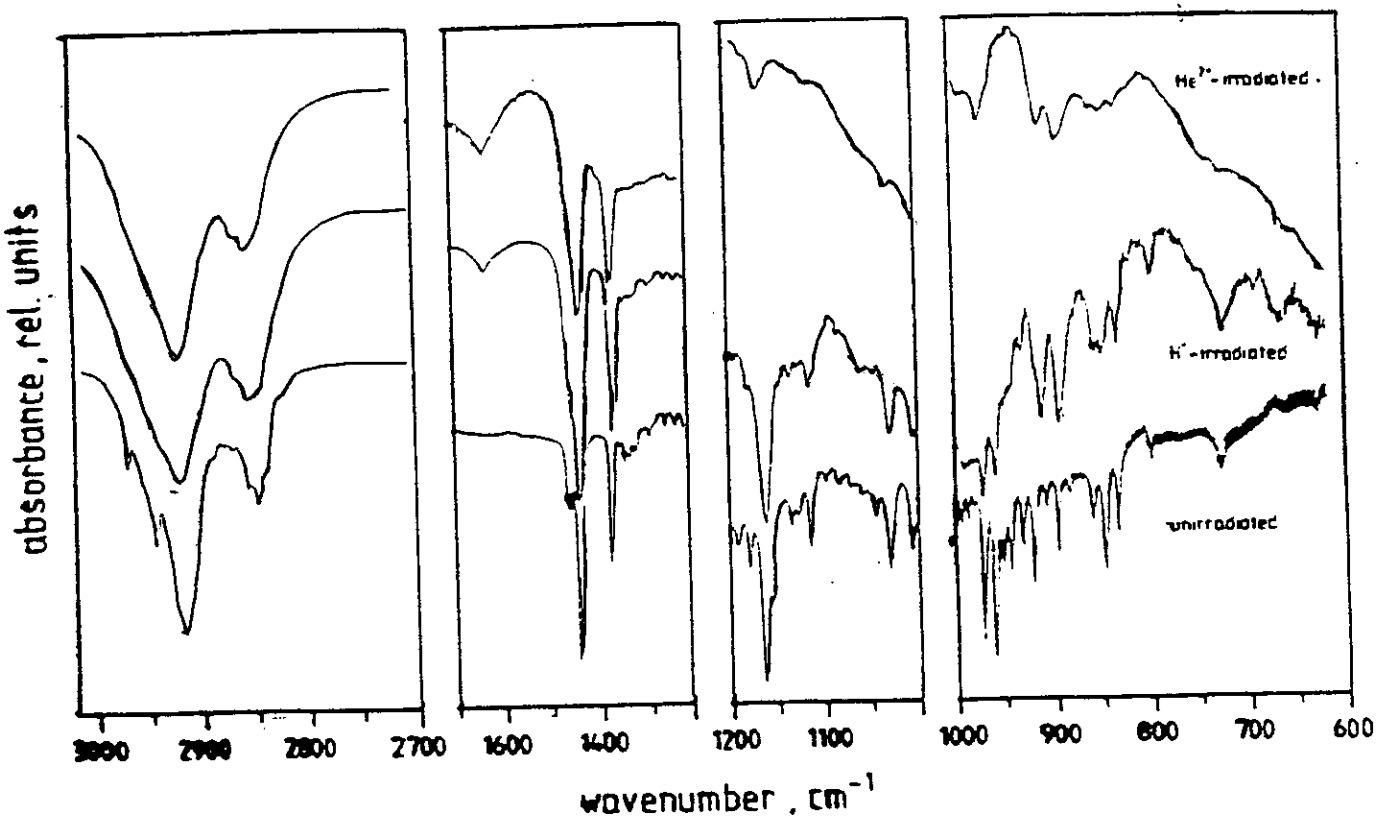

Fig. 22 : Details of FT-IR spectrum of androstane in transmission at maximum dose of H^+ and $^4He^{2+}$ ions compared with that of the unirradiated sample.

Table 12 : Wavenumbers of original and new bands in androstane with assignment of vibration mode, its strength and FWHM.

position cm^{-1}	old or new bands after irradiation	vibration mode	FWHM cm^{-1}	relative strength*
3420	H^+		240	s
3420	$^4He^{2+}$	ν(O-H) stretching	270	s
2960	old	ν_{as} ($-CH_3$)	2	s
2945	old		3	s
2920	old	ν_{as} ($-CH_2$)	15	m
2870	old	ν_{s} ($-CH_3$)	0.5	m
2850	old	ν_{s} ($-CH_2$)	13	s
1720	H^+	ν (C=O)	2	vw
1720	$^4He^{2+}$		3	vw
1635	H^+	ν (C=C) stretching	54	m
1635	$^4He^{2+}$		60	m
1448	old/H^+/He^{2+}	δ ($-CH_2$) + δ_{as} ($-CH_3$)	42	s
1378	old/H^+/He^{2+}	δ_s($-CH_3$)	16	s
1200-700	old	various ring skeleton modes		vw-m
990	H^+	δ(C-H) in -CH = CH2	9	vw
990	$^4He^{2+}$		9	vw
980	H^+	δ_{op} (C-H) in - CH = CH-	60	m
980	$^4He^{2+}$	or ring vibration	50	m
910	H^+	δ_{op} (CH_2), -CH = CH_2	13	w
910	$^4He^{2+}$		19	w
688	H^+		5	vw
665	H^+	δ_{op} (C-H) in - CH = CH-, inside ring	23	w
669	$^4He^{2+}$		6	vw

* s = strong, m = medium, w = weak, vw = very weak

Table 13 : Integrated area of selected peaks (old and new) of androstane at different doses for H^+ and $^4He^{2+}$ Ion Irradiation.

Ion irradiation	dose eV/Catom	peak position,cm^{-1}									
		2960	1630	1448	1378	980	970	910	724	669	665
H^+	0	1.29		3.44	1.25	0.35	0.16		0.20		
	1.4	1.43	0.46	6.24	2.46	0.44	0.17	0.01	0.15		0.01
	2.8	0.51	1.59	6.97	2.65	0.67	0.06	0.07	0.26		0.11
	5.7	0.22	1.42	7.21	2.78	0.85	0.05	0.17	0.31		0.13
$^4He^{2+}$	9.8	0.17	1.37	5.23	3.19	0.72	0.11	0.31	0.09	0.11	0.11
	19.6		3.61	5.84	3.60	0.65	0.08	0.34	0.05	0.08	0.08
	38.1		4.5	6.51	4.61	0.72	0.13	0.45	0.03	0.01	0.01

Table 14 : Bond ratios of radiation products of androstane for H^+ and $^4He^{2+}$ ion irradiation at maximum dose.

bond ratios		
androstane	H^+	$^4He^{2+}$
$\frac{N(-\overset{1}{C}=\overset{1}{C}-)}{N(-\underset{1}{\overset{1}{C}}-)}$	0.03	0.02
$\frac{N(-\overset{1}{C}=C\diagdown^{\prime})}{N(-CH_3)}$	6.10^{-3}	10^{-2}
$\frac{N(-\overset{1}{C}=C-)}{N(-\underset{1}{\overset{1}{C}}=C\diagdown^{\prime})}$	2.7	2.2

Fig. 23 exhibits the spectra of naphthalene between 4000 and 400 cm^{-1} for the different sources of radiation : H^+, $^3He^{2+}$and $^4He^{2+}$ ions in comparison with that of the unirradiated sample. It seems that naphthalene suffered a general decrease of the intensity of all FTIR bands, however it did not show formation of distinct new band systems. Table 15 lists the position of the old bands, the vibration modes and the relative band strength.

Another polycyclic aromatic hydrocarbon molecule is anthracene. Fig. 24 shows the FTIR spectra in transmission at maximum dose of H^+, $^3He^{2+}$ and $^4He^{2+}$ ion irradiation (5.0, 13.6 and 42 eV/C atom, respectively) with that of the unirradiated sample. It shows that no massive changes occur, except that few weak bands are found between 1800 and 1200 cm^{-1}. Fig 25 shows some of the bands on a larger scale. It can be seen that a new feature appears at $\simeq$ 1620 cm^{-1} (6.17 μm), 1673 cm^{-1} (5.98 μm) and 1590 cm^{-1}(6.29 μm) for H^+, $^3He^{2+}$ and $^4He^{+2}$ ion irradiation, due to ring vibration only for $^3He^{2+}$ irradiation appears a feature at $\simeq$ 1310 cm^{-1} (7.63 μm) which is due to ring vibration. For $^4He^{2+}$ irradiation a new feature appears at 1182 cm^{-1} (8.86 μm) which is due to ring vibration. Table 16 shows the disapp-arition of the old and the rise of new bands of anthracene. Table 17 shows the integrated area of selected peaks (old and new) for different doses.

III-1.2.2 Kerogen :

Fig. 26 shows the effects of maximum dose H^+ and $^4He^{2+}$ ion irradiation (27.6 and 189 eV/C atom, respectively) of kerogen. It can be seen that no massive changes occur, except that few weak bands appeared (S- and O- bands) between 1000 and 1500 cm^{-1}. For H^+ irradiation there appears new features at 1027 cm^{-1} and 1094 cm^{-1}. For $^4He^{2+}$ ion irradiation there appear three new features at 1025 cm^{-1} due to S=O, 1094 cm^{-1} and 1400 cm^{-1}. It was noticed that the old band at 715 cm^{-1}

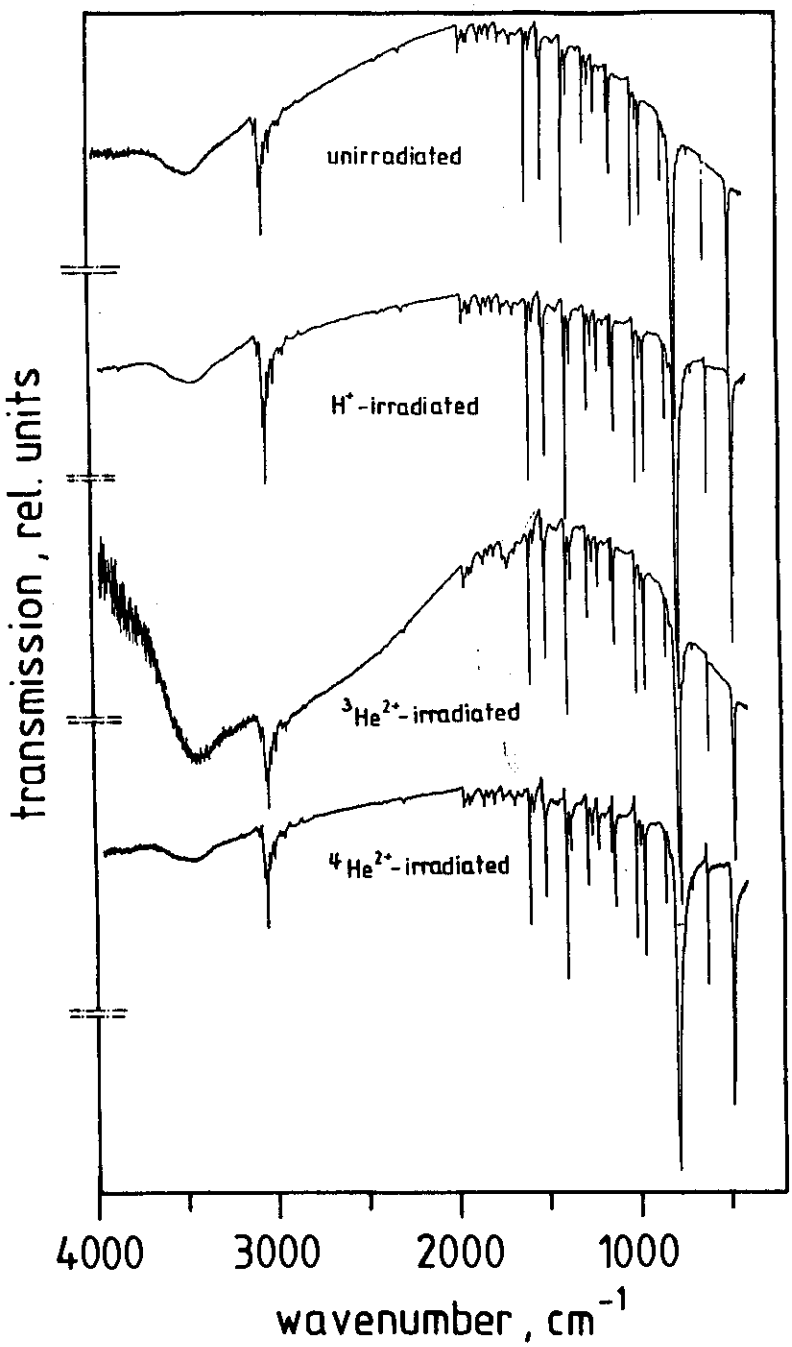

Fig. 23 : Comparison of FT-IR spectrum of naphthalene in transmission at a maximum dose of H^+, $^3He^{2+}$ and $^4He^{2+}$ ions (6.2, 13.6 and 33.4 eV per carbon atom, resp.) with unirradiated sample.

Table 15 : The wavenumber of old and new bands after irradiation of naphthalene with assignment of vibration mode and its strength.

position cm^{-1}	vibration mode	relative strength*
3420	ν (O-H) stretching (old)	m
3067		w
3062		m
3050	ν (= C ↔ H) stretching (old)	vs
3029		m
3002		m
1593	ν (C = C) stretching (old)	vs
1505		s
1395		vs
1270	ν (C - C) stretching (old)	s
1209		m
1123		w
959		s
845		vw
798	δ (C -H) wagging deformation (old)	w
780		vs
617		s
480	ring deformation (old)	s
470		s

* s = strong, m = medium, w = weak, vw = very weak, vs = very strong

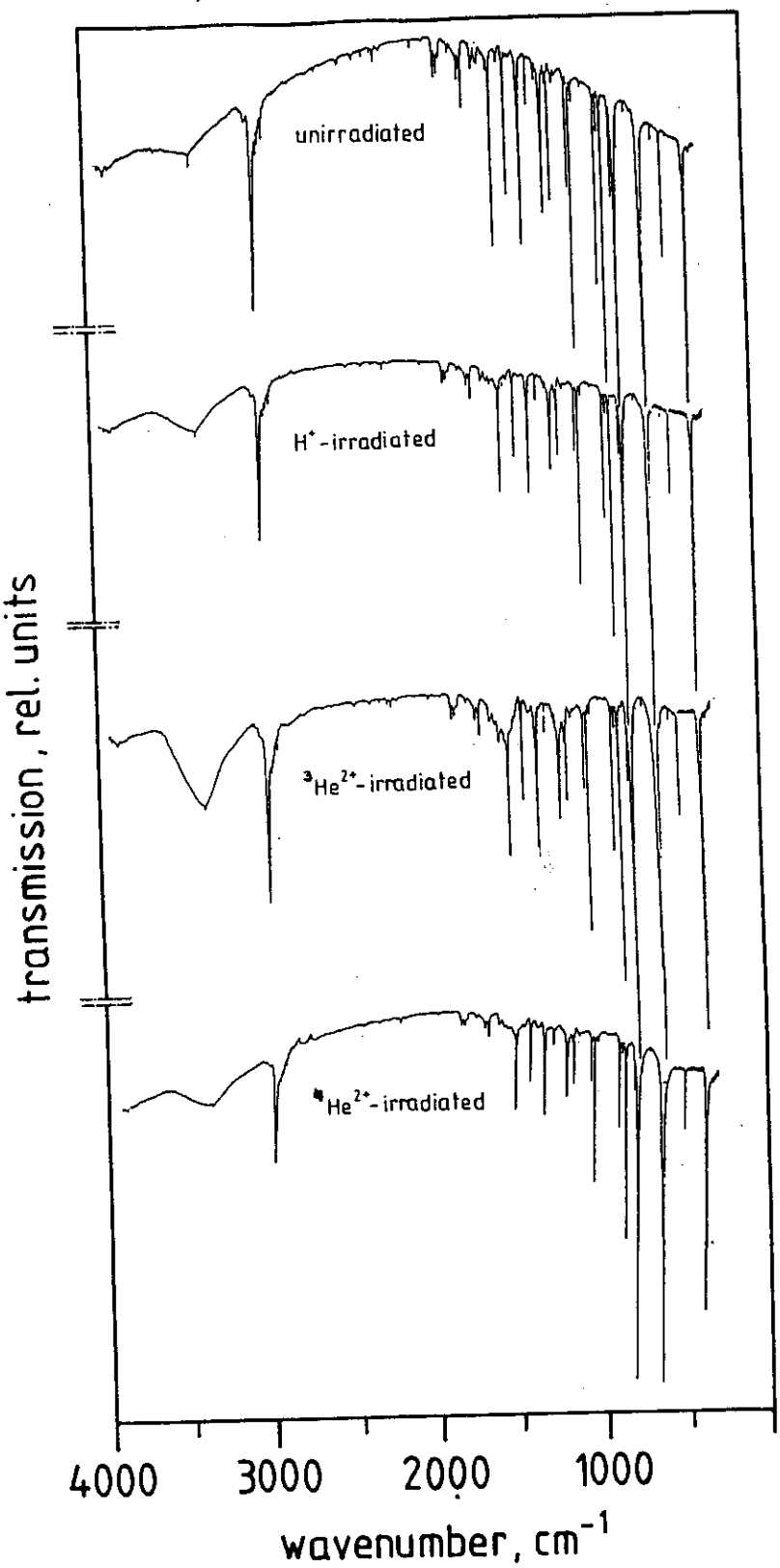

Fig. 24 : Comparison of FT-IR spectrum of anthracene in transmission at maximum dose of H^+, $^3He^{2+}$ and $^4He^{2+}$ ions (5.0, 13.6 and 42 eV per carbon atom, resp.) with that of the unirradiated sample.

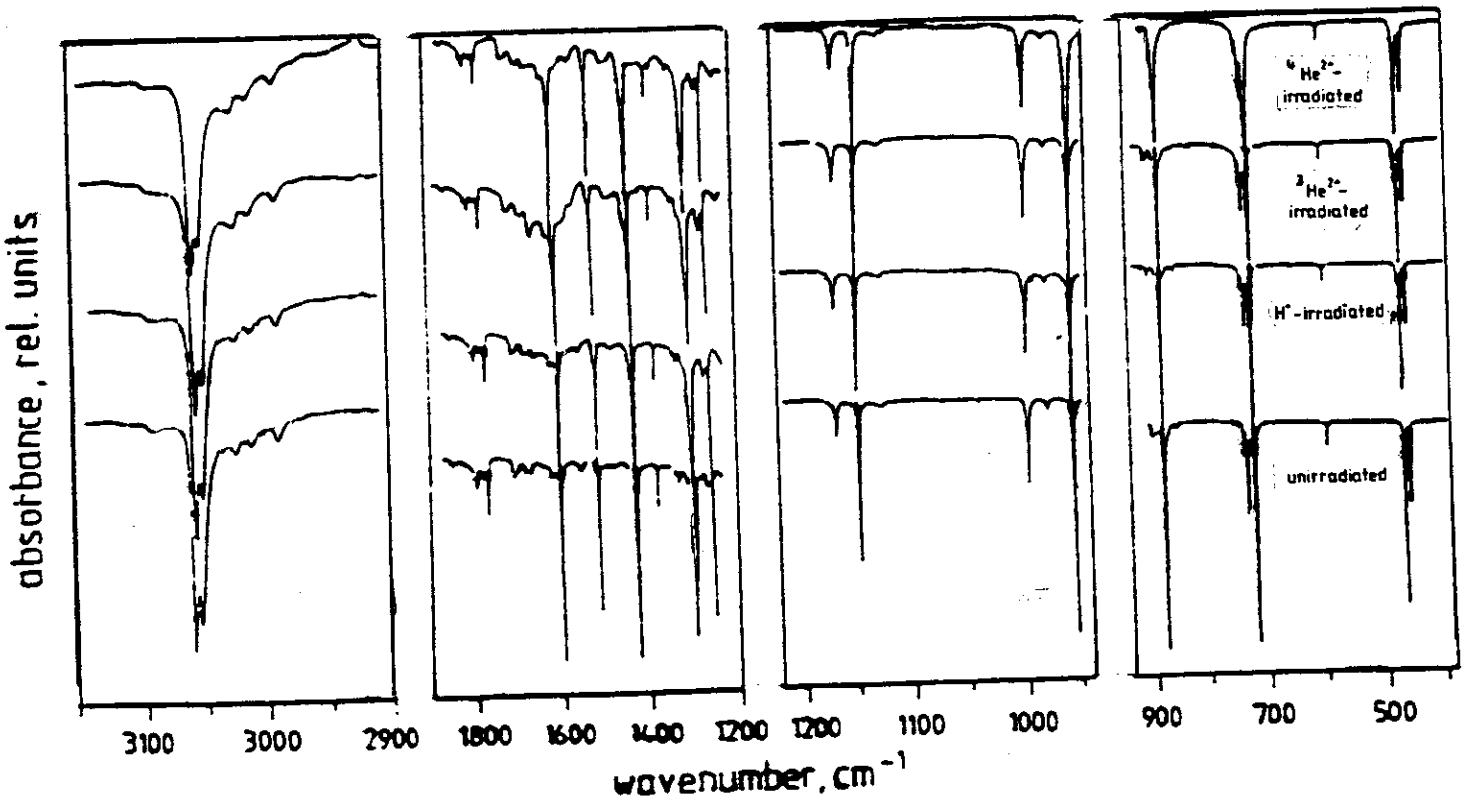

Fig. 25 : Development of FT-IR spectrum of anthracene at maximum dose of H^+, $^3He^{2+}$ and $^4He^{2+}$ ions compared to that of the unirradiated sample.

Table 16 : Wavenumbers of old and new bands after irradiation of anthracene with assignment of vibration mode, its strength and FWHM.

position cm^{-1}	old or new bands after irradiation	vibrational mode	FWHM cm^{-1}	relative strength*
3420	H^+	ν(O-H) stretching	181	s
3420	$^3He^{2+}$		212	s
3420	$^4He^{2+}$		116	s
3080	old	ν(= C ↔ H)	10.5	w
3055	old		5.2	s
3050	old		5.2	m
3023	old		7.0	w
3010	old		5.0	w
2988	old	ν(C = C) of open chain molecule (cis)	8.1	w
1673	H^+		5.5	vw
1673	$^3He^{2+}$		11.0	vw
1673	$^4He^{2+}$		2.2	vw
1620	old	ring vibration	1.1	s
~1620	H^+		66	w
~1620	$^3He^{2+}$		88	m
~1620	$^4He^{2+}$		77	w
1602	$^3He^{2+}$		5.2	vw
1602	$^4He^{2+}$		3.0	vw
1590	H^+		1.1	vw
1590	$^3He^{2+}$		2.5	vw
1590	$^4He^{2+}$		1.1	vw
1534	old		5.5	s
1495	$^3He^{2+}$		11	vw
1495	$^4He^{2+}$		10	vw
1480	$^3He^{2+}$		1.1	vw
1480	$^4He^{2+}$		2.0	vw
1445	old		9.0	s
1422	$^4He^{2+}$		2.2	vw
1422	$^4He^{2+}$		2.2	vw
1380	$^3He^{2+}$		3.3	w
1310	H^+		1.1	w
1310	$^4He^{2+}$		1.1	vw
1310	$^4He^{2+}$		1.1	vw
1182	$^3He^{2+}$		0.5	vw
1182	$^4He^{2+}$		0.2	vw
1146	old		1.1	s
884	old	C-H wagging deformation	6.0	vs
745-730	old		35	vs
475	old	ring deformation	7.0	vs

* s = strong, m = medium, w = weak, vw = very weak, vs = very strong

Table 17: Integrated areas of selected peaks (old and new) of anthracence at different doses for H^+,$^3He^{2+}$ and $^4He^{2+}$ Ion irradiation

ion irradiation	dose eV/C-atom	peak position, cm^{-1}					
		1673	1620	1590	1182	1448	475
H^+	0		1.96			2.85	9.61
	1.2	0.05	1.61	0.02		2.54	8.76
	2.4	0.07	1.28	0.03		2.09	7.63
	5.0	0.08	0.95	0.03		1.36	5.14
$^3He^{2+}$	3.4	0.08	1.48	0.03		2.61	8.53
	6.8	0.26	1.47	0.04		2.19	7.20
	13.6	0.40	1.42	0.06		2.15	6.22
$^4He^{2+}$	8.4	0.02	0.79	0.01	0.015	1.33	5.91
	16.8	0.03	0.87	0.02	0.016	1.58	5.65
	42.0	0.05	0.64	0.02	0.018	1.06	3.31

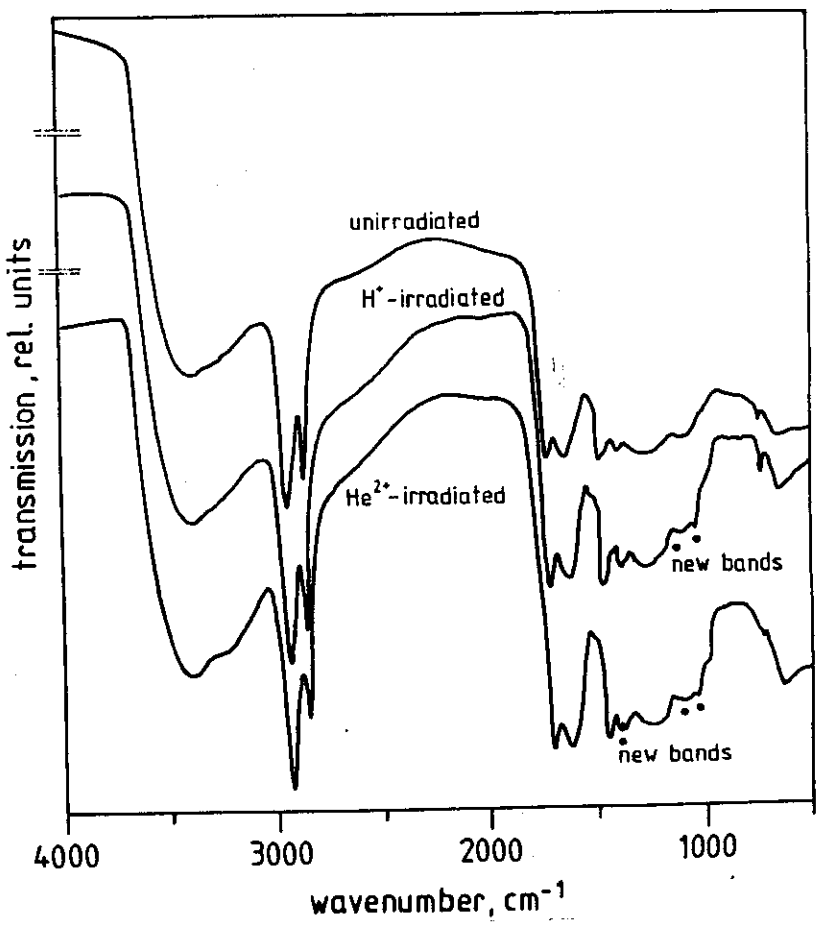

Fig. 26 : Comparison of FT-IR spectrum of kerogen in transmission at maximum dose of H^+ and $^4He^{2+}$ ions (27.6 and 189 eV per carbon atom, resp.) with that of the unirradiated sample.

(skeleton vibration) somewhat disappeared for H^+ and $^4He^{2+}$ ion irradiation. Table 18 lists the wavenumbers of old and new bands with assignment of the vibration mode and its relative band strength. Moreover, Table 19 shows the integrated area of selected peaks of naphthalene and kerogen at different doses.

III-1.2.3 Thin Organic Layers on Minerals :

The changes induced in the organic thin layers on mineral grains after the irradiation by 20 MeV H^+ ions were monitored by infrared spectroscopy in diffuse reflectance. Fig. 27 compares the transmission spectra of pure pentlandite at maximum proton dose with that of unirradiated pentlandite. It can be seen that few new bands appear : a broad peak at 3400, a medium peak at 1630, a very weak peak at 1400, a weak peak at 1150, medium peak at 1000, 700 and 450 cm^{-1}. Increase of some old bands at 1100, 1050 and 600 cm^{-1} was observed. The same figure contains also the spectra of pentlandite with tetracosane layer. It can be noticed that no massive changes can be observed due to the low resolution of the weak bands of the organic substance.

III-1.3 Gaschromatography :

The results of the analysis by gaschromatography GC-FID after irradiation by cyclotron ions of five high molecular hydrocarbons proved fragmentation. Fig. 28 exhibits the effects of different doses of H^+ and $^3He^{2+}$ ion irradiation on the rest gas chromatogram of tetracosane. New hydrocarbons show up containing up to six and eight carbon atoms (C_6, C_8). To compare the new fragments with different doses of H^+ we can say that the strongest GC peaks were C_6 and C_8 attributed to branched C_6 (isohexane, isohexene) and n-octane, respectively. Some smaller hydrocarbon peaks increased with the radiation dose, such as n-pentane (C_5H_{12}), n-hexane (C_6H_{12}) and 1-heptene (C_7H_{14}). From the comparison of the new fragments with different doses

Table 18 : Wavenumber of old and new bands after irradiation of kerogen with assignment of vibration mode and its strength.

position cm^{-1}	old or new bands after irradiation	vibration mode	relative strength*
3400		ν (0-H) stretching	s
2926	old	ν (C-H) stretching	s
2850	old		s
1700	old	ν (C = 0) stretching	s
1610	old	ν (C = C) stretching	s
1450	old	δ(C-H) deformation in CH_2, CH_3	m
1400	$^4He^{2+}$		m
1378	old		m
~ 1200	old	δ(C-H) in H-C = ?	w
1094	H^+	S = O	vw
1094	$^4He^{2+}$		
1027	H^+		
1025	$^4He^{2+}$		w
715	old	skeleton vibration	w

* s = strong, m = medium, w = weak, vw = very weak

Table 19 : Integrated area of selected peaks of naphthalene and kerogen at different doses for different kinds of irradiation.

ion irradiation	naphthalene		kerogen	
	dose eV/C atom	peak at 475 cm^{-1}	dose eV/C atom	peak at (1710-1627) cm^{-1}
H^+	0	5.49	0	70.2
	1.2	4.92	6.9	55.4
	2.4	4.62	13.8	46.5
	6.2	3.01	27.6	41.7
$^3He^{2+}$	3.14	5.52		
	6.8	5.30		
	13.6	5.10		
$^4He^{2+}$	8.4	5.60	47.3	57.2
	16.8	5.51	94.6	62.2
	33.4	5.55	189.0	70.1

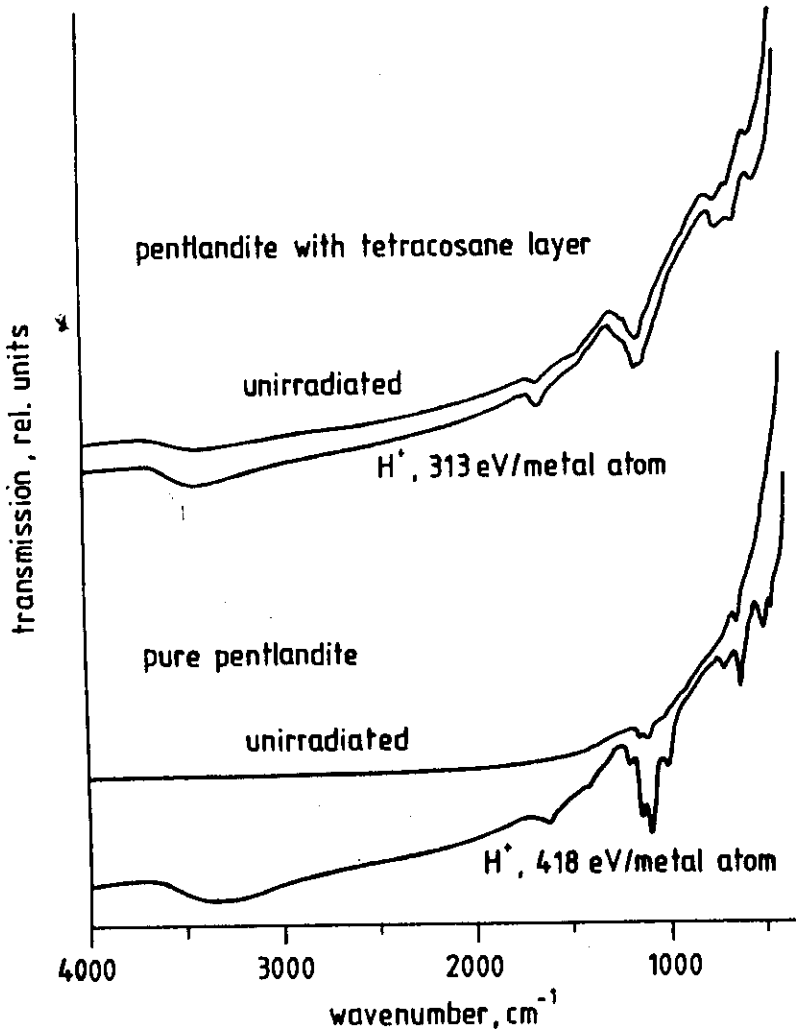

Fig. 27 : FT-IR spectra in diffuse reflectance; the upper two spectra show pentlandite with tetracosane layer unirradiated and pentlandite with tetracosane layer at high dose H^+ ions (313 eV/ metal atom); the lower two spectra show pure pentlandite unirradiated and pure pentlandite at high dose H^+ ions (418 eV / metal atom).

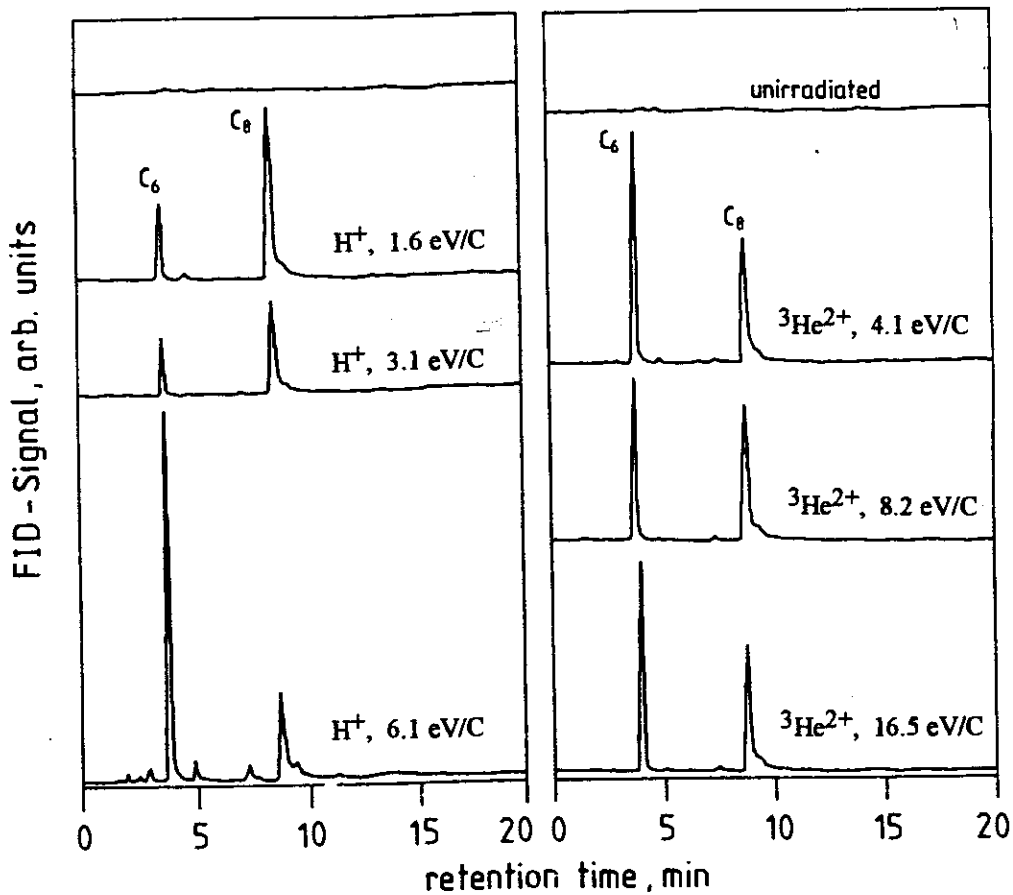

Fig. 28 : Comparison of GC chromatograms of tetracosane after different doses of H^+ and $^3He^{2+}$ ions with that of the unirradiated sample.

of $^3He^{2+}$ ions it becomes obvious that the strongest GC peaks were C_6 and C_8. Their amount remains nearly the same with the radiation dose.

The analysis of androstane by GC exhibits much more changes. Fig. 29 compares the GC chromatograms of androstane at different doses of H^+ and $^4He^{2+}$ ion irradiation with that of the unirradiated sample. It can be seen that major fragments contain six and eight carbons (C_6 and C_8). There is, however, a relatively broad peak system beyond C_8 which may contain C_{10} and higher. There are peaks of some smaller hydrocarbons such as C_4. Their amount obtains a maximum at a dose of 2.8 eV/C atom of H^+ ions. At high dose (5.7 eV/C atom) of H^+ the main peak C_6 decreases and C_8 disappears totally. At the same dose occurs an increase of C_4. In case of $^4He^{2+}$ ion irradiation at a dose of 9.8 eV/C atom $^4He^{2+}$ two major peaks of C_6 and C_8 show up with small fragments at C_4.

The analysis by GC of polycyclic aromatic hydrocarbons such as naphthalene yields different kinds of radiation fragments containing up to ten carbon atoms (C_{10}). Fig. 30 shows the effects of different doses of H^+ and $^4He^{2+}$ ion irradiation on chromatograms. It exhibits few very small peaks accompanying the original peak of naphthalene, characteristic for fragments such as C_6 and C_7 (benzene and toluene).

Fig. 31 compares the GC chromatograms of anthracene at different doses for various kinds of radiation with that of the unirradiated sample. Some fragments contain up to ten carbon atoms (C_{10}), a small peak at C_6 is due to benzene, a strong peak at C_7 is due to toluene and a relatively strong peak at C_{10} due to naphthalene ($C_{10}H_8$). Their amounts decrease with the radiation dose accompanied by a relative increase of C_6. In the case of $^3He^{2+}$ and $^4He^{2+}$ ion irradiation the new fragments are less pronounced.

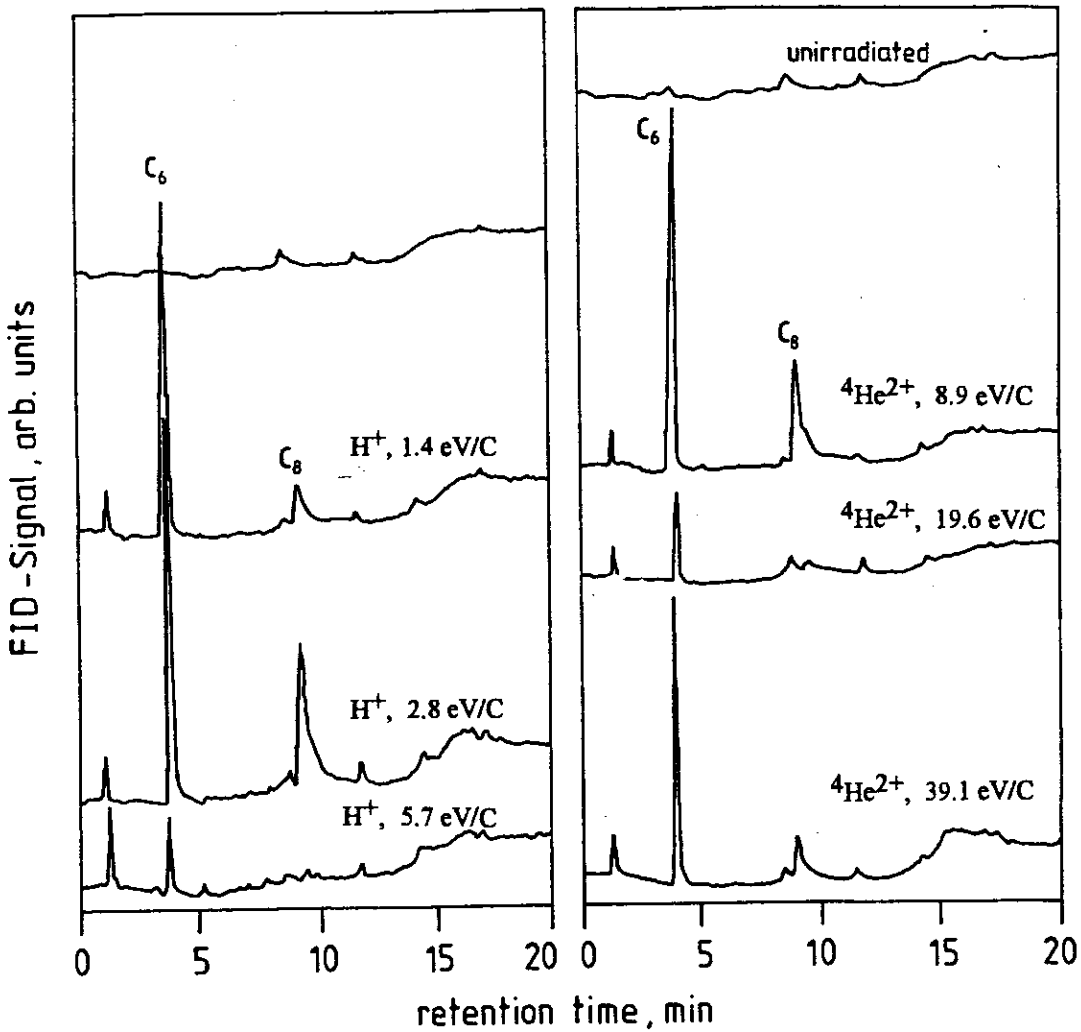

Fig. 29 : Comparison of GC chromatogram of androstane after different doses of H^+ and $^4He^{2+}$ ions with that of the unirradiated sample.

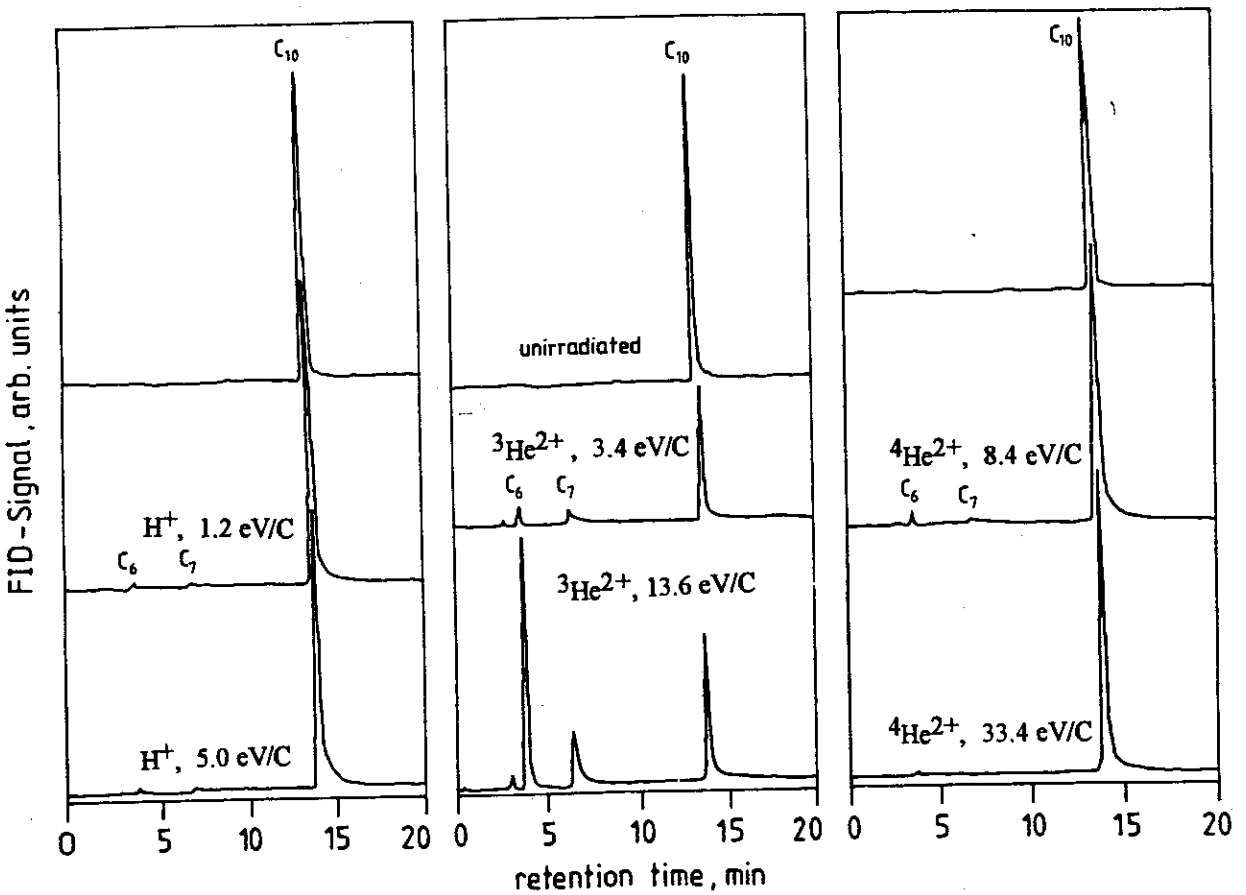

Fig. 30 : Comparison of GC chromatograms of naphthalene after different dose of three kinds of radiation with that of the unirradiated sample.

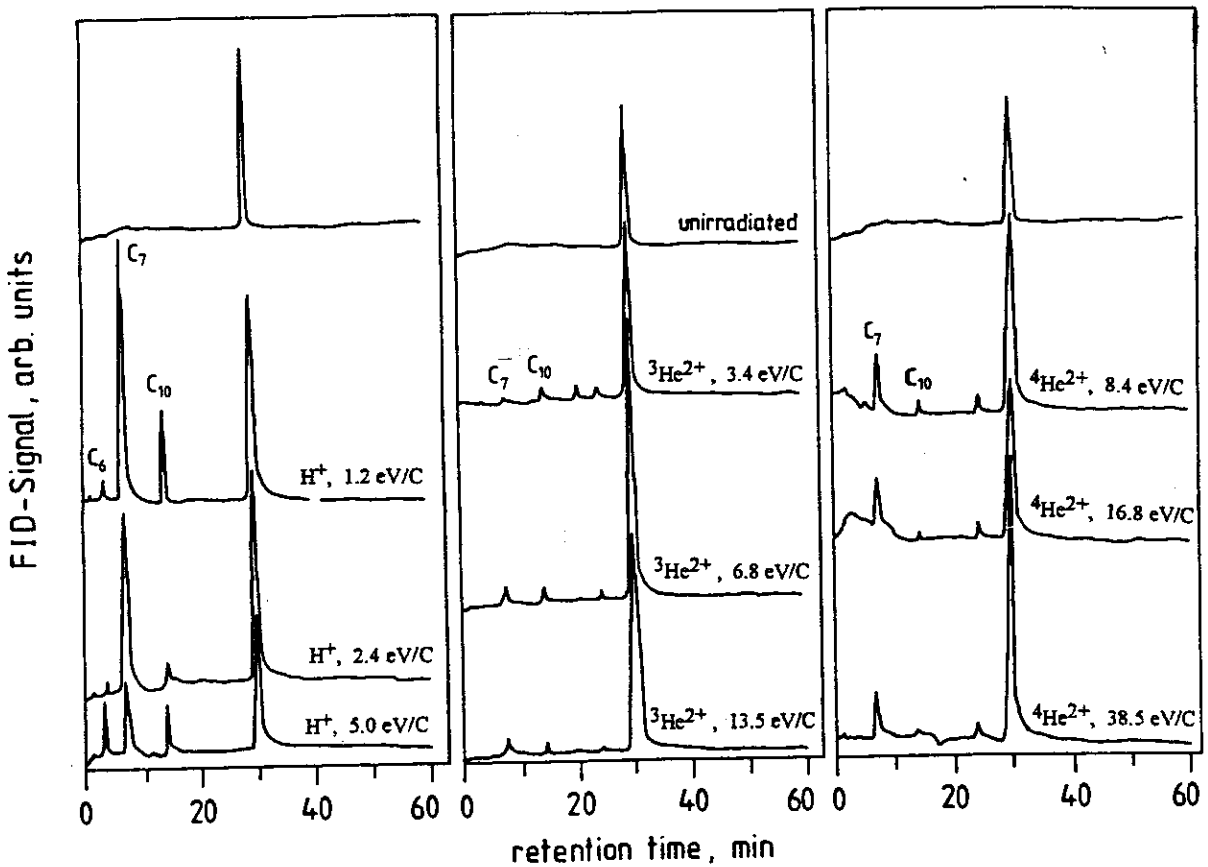

Fig. 31 : Comparison of GC chromatograms of anthracene after different doses of various kinds of radiation with that of the unirradiated sample.

The analysis of kerogen by GC after H^+ and $^4He^{2+}$ ion irradiation shows that the majority of fragments range from C_4 to C_{10}. Fig. 32 shows the effects of different doses of H^+ and $^4He^{2+}$ ions on chromatogram. It seems that for H^+ ion irradiation at low doses the main peaks are C_6 and C_8 and a very small peak at C_4. But at 13.8 eV/C atom the main peak at C_6 decreases and many fragments of hydrocarbons show up ranging from C_4 to C_{10} and higher. These fragments are formed preferentially at high radiation dose. The irradiation of kerogen by $^4He^{2+}$ ion gives different results. At 47.3 eV/C atom, the strongest peak is of C_6 and small peaks of C_4 and C_8.

III-2 Consequences of Vacuum Ultraviolet Irradiation :

III-2.1 Visual Inspection of Samples :

No change was observed for pure organic hydrocarbons (tetracosane and androstane) as thin layers on minerals as siderite with tetracosane, siderite with androstane, pentlandite with tetracosane, pentlandite with androstane, pyrrhotine with tetracosane and pyrrhotine with androstane by visual inspection.

III-2.2 Fourier Transform Infrared Spectroscopy in Diffuse Reflectance :

III-2.2.1 Pure Organic Substances :

8 h of VUV irradiation of the pure organic hydrocarbons, tetracosane and androstane, did not yield any new bands as shown in Fig. 33 & Fig. 34, respectively.

III-2.2.2 Thin Organic Layers on Minerals :

Five molecular layers of tetracosane and androstane on mineral grains of siderite, pentlandite and pyrrhotine were irradiated by VUV light at 100-300 nm. Figures 35-39 show the infrared spectra in diffuse reflectance of pure mineral, of mineral with a thin layer of organic substance on it, unirradiated and irradiated at

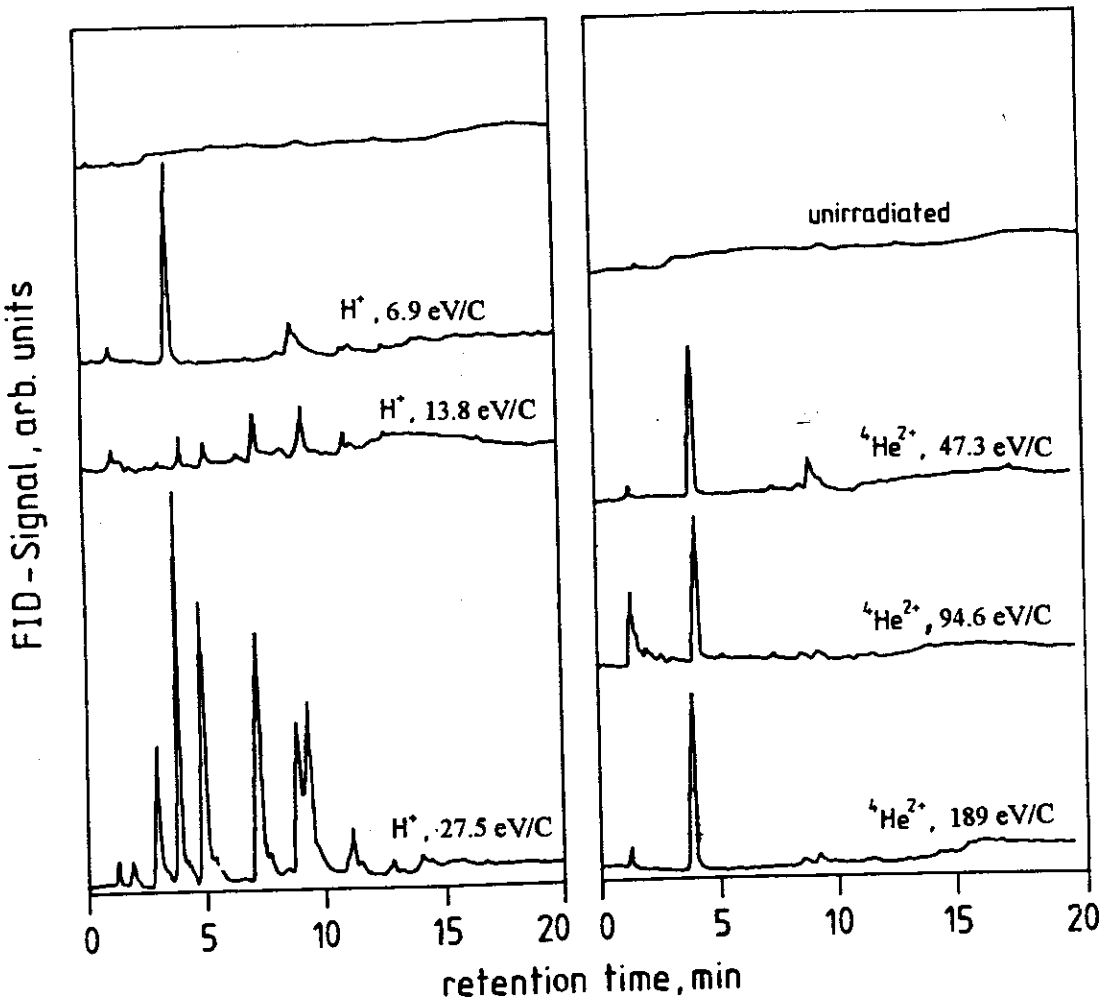

Fig. 32 : Comparison of GC chromatograms of kerogen after different doses of H^+ and $^4He^{2+}$ ions with that of the unirradiated sample.

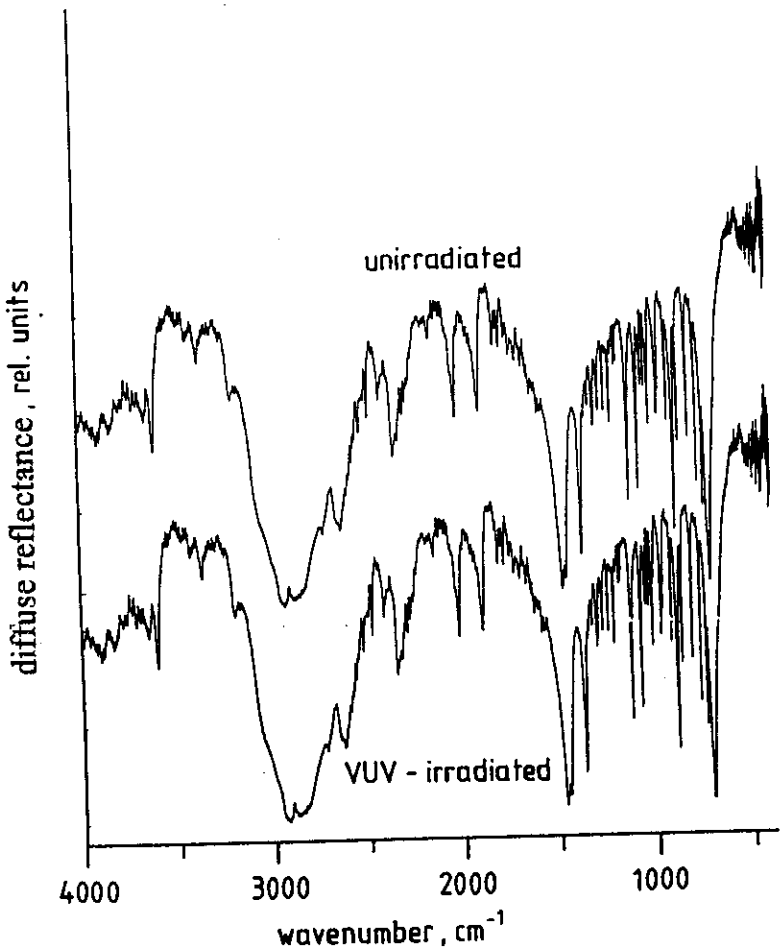

Fig. 33 : FT-IR spectrum in diffuse reflectance of tetracosane at 80 K after irradiation for 8 h with VUV photons.

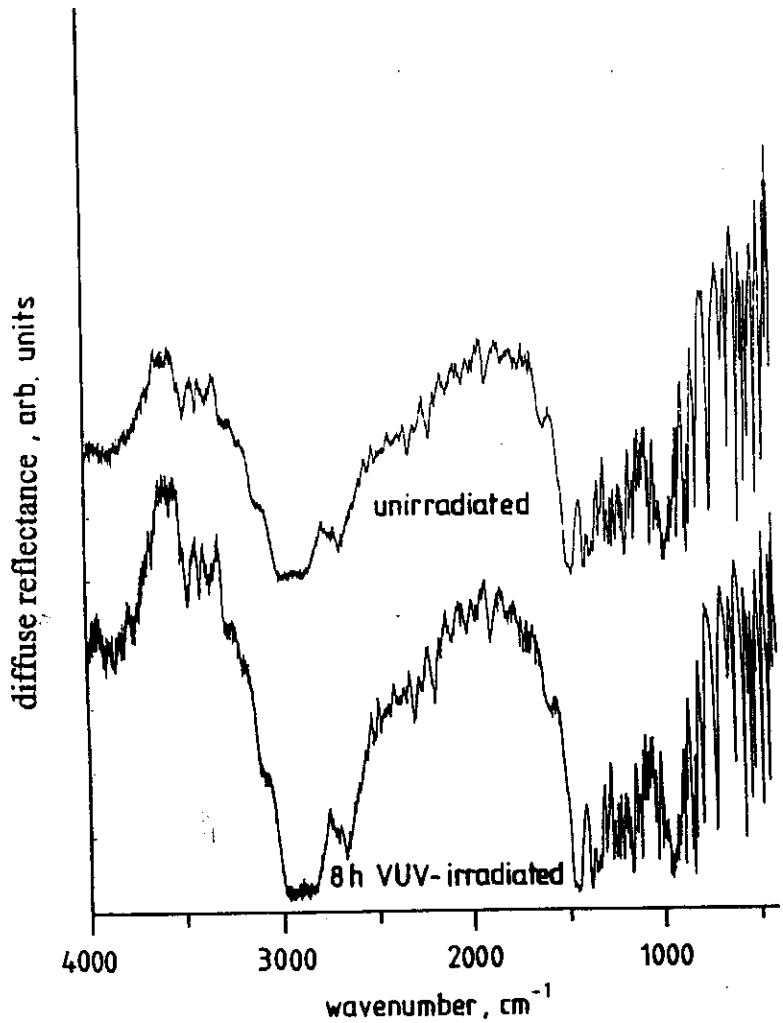

Fig. 34 : FT-IR spectrum in diffuse reflectance of androstane at 80 K after irradiation for 8 h with VUV photons.

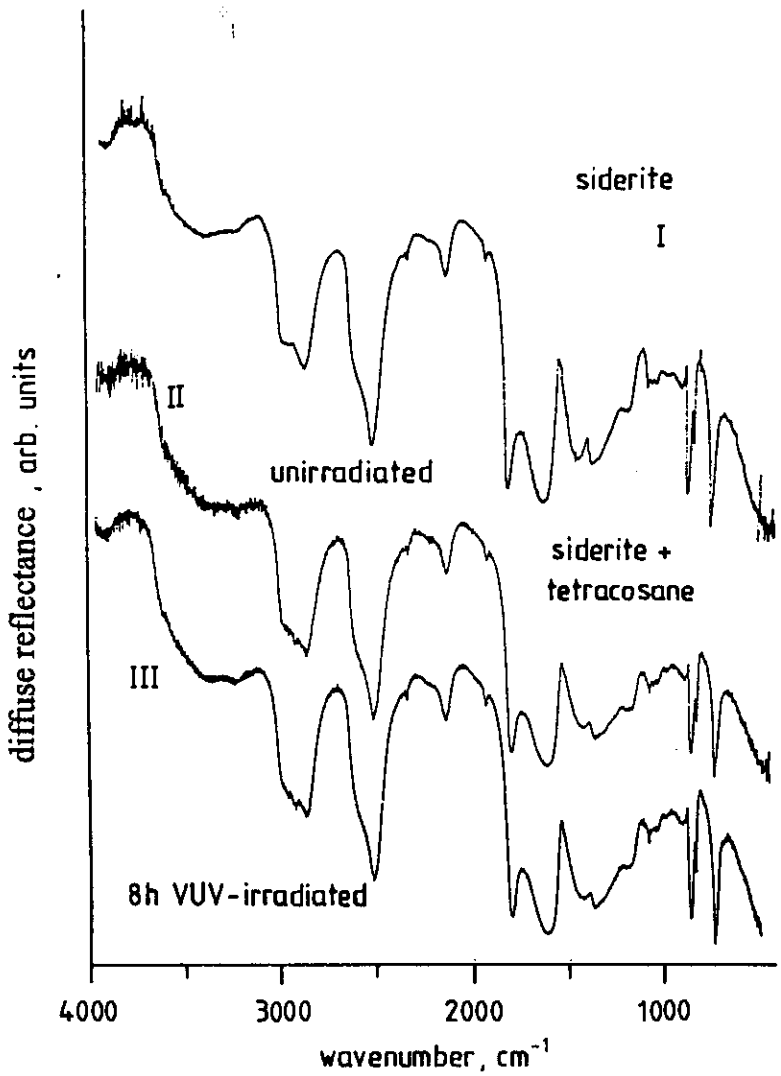

Fig. 35 : FT-IR spectrum in diffuse reflectance to compare
I- pure siderite
II- siderite + tetracosane unirradiated and
III- siderite + tetracosane at 80 K irradiated for 8 h with VUV photons.

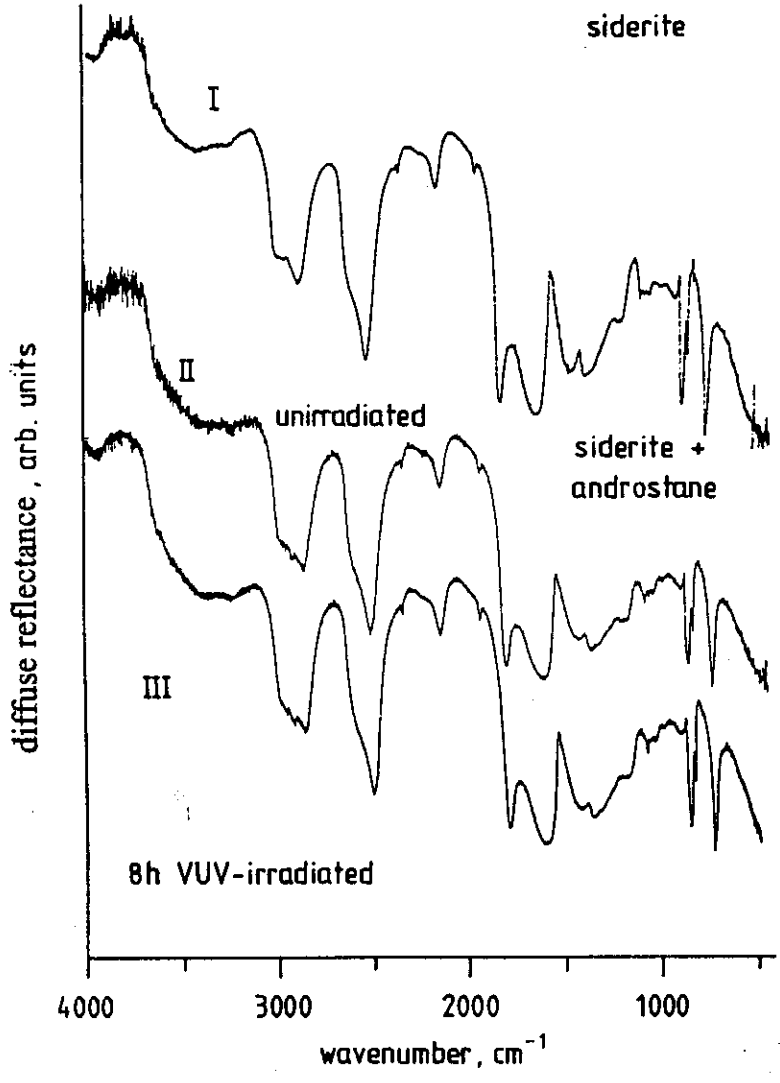

Fig. 36 : FT-IR spectrum in diffuse reflectance to compare
I- pure siderite
II- siderite + androstane unirradiated and
III- siderite + androstane at 80 K irradiated for 8 h with VUV photons.

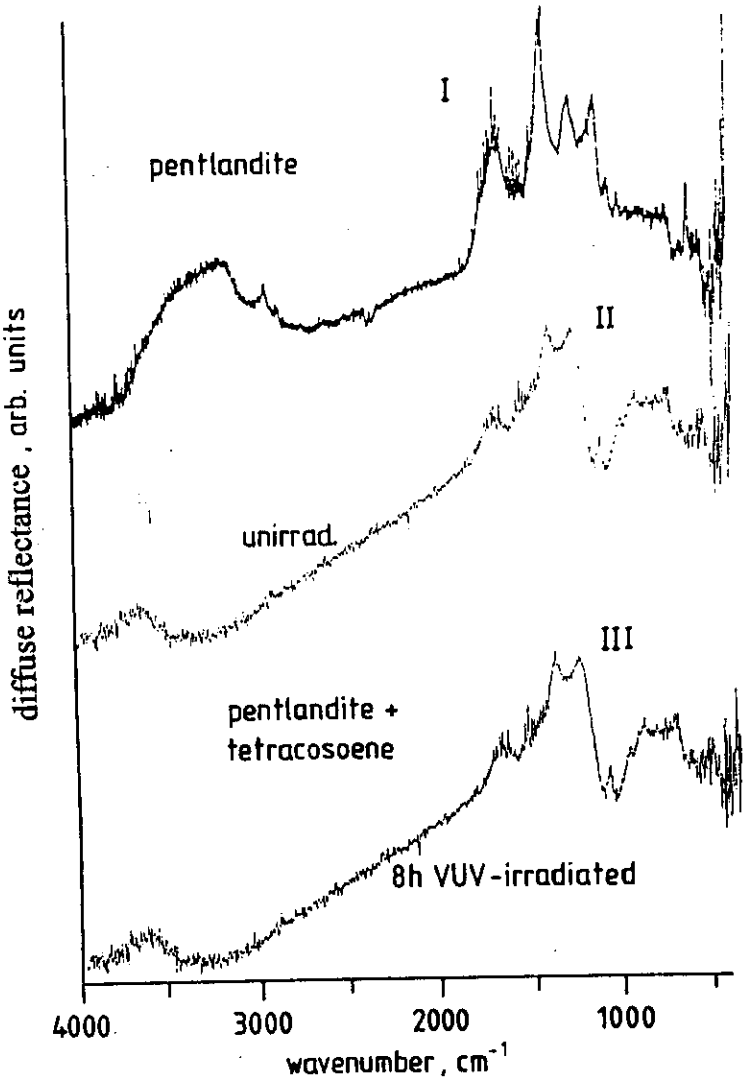

Fig. 37 : FT-IR spectrum in diffuse reflectance to compare
I- pure pentlandite
II- pentlandite + tetracosane unirradiated and
III- pentlandite + tetracosane irradiated at 80 K for 8 h with VUV photons.

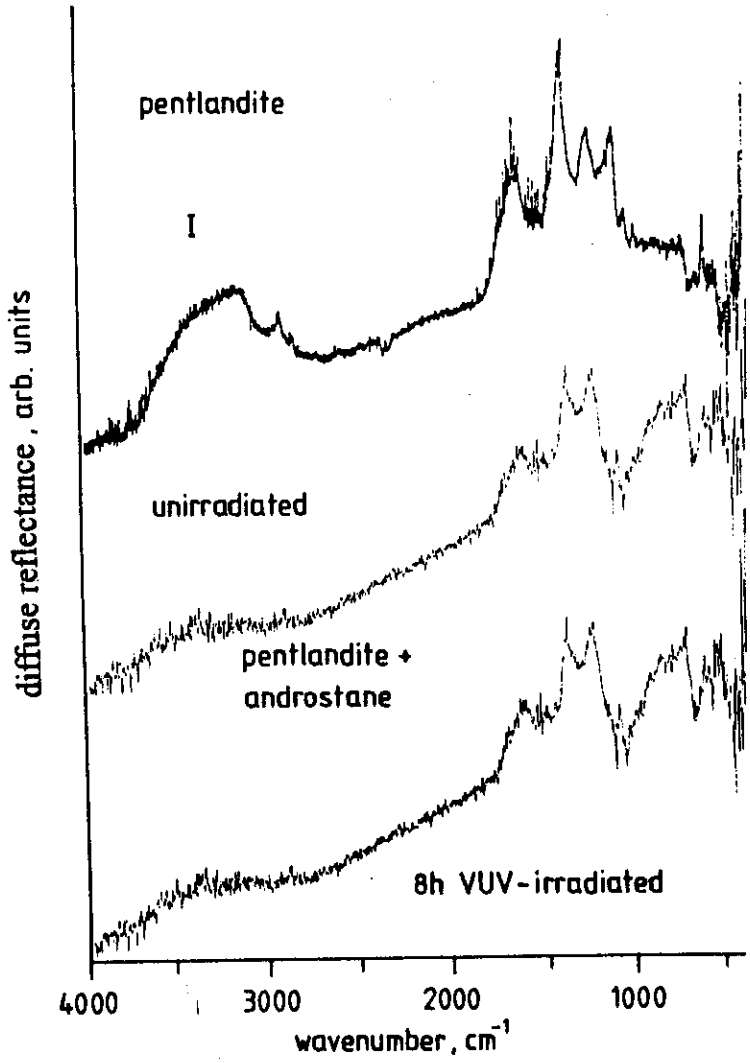

Fig. 38 : FT-IR spectrum in diffuse reflectance to compare :
I- pure pentlandite
II- pentlandite + androstane unirradiated and
III- pentlandite + androstane irradiated at 80 K for 8 h with VUV photons.

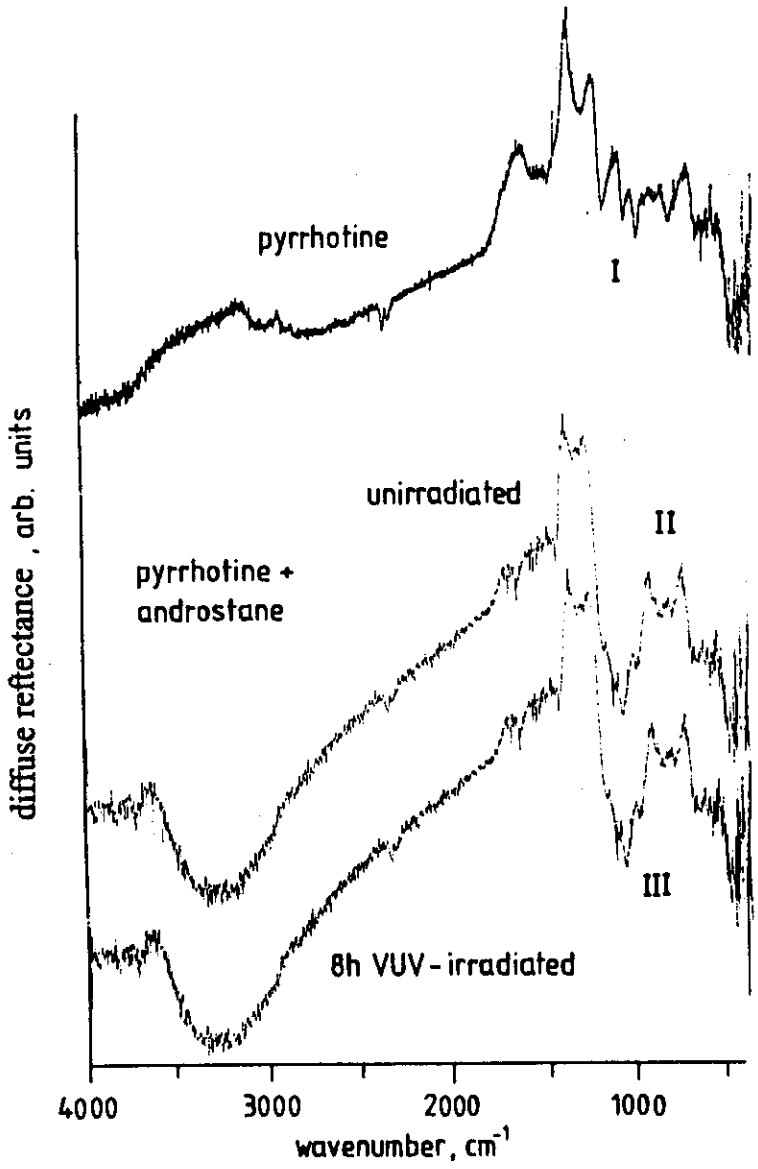

Fig. 39 : FT-IR spectrum in diffuse reflectance to compare :
I- pure pyrrhotine
II- pyrrhotine + androstane and
III- pyrrhotine + androstane irradiated at 80 K for 8 h with VUV photons.

77 K for 8h. A destruction of organic molecules even at relatively high fluences of 130 eV/ metal could not be observed.

III-2.3 Gaschromatography :

The results of the analysis by gaschromatography after heating of pure organic hydrocarbons as tetracosane and androstane which were irradiated at 77 K for 8h with VUV photons are displayed in Fig. 40 & 41. Since the new peaks of C_6 and C_8, but also of other species are very weak, the magnification of resolution causes enormous background noise. Thus, it is relatively difficult to obtain quantitative results on product formation.

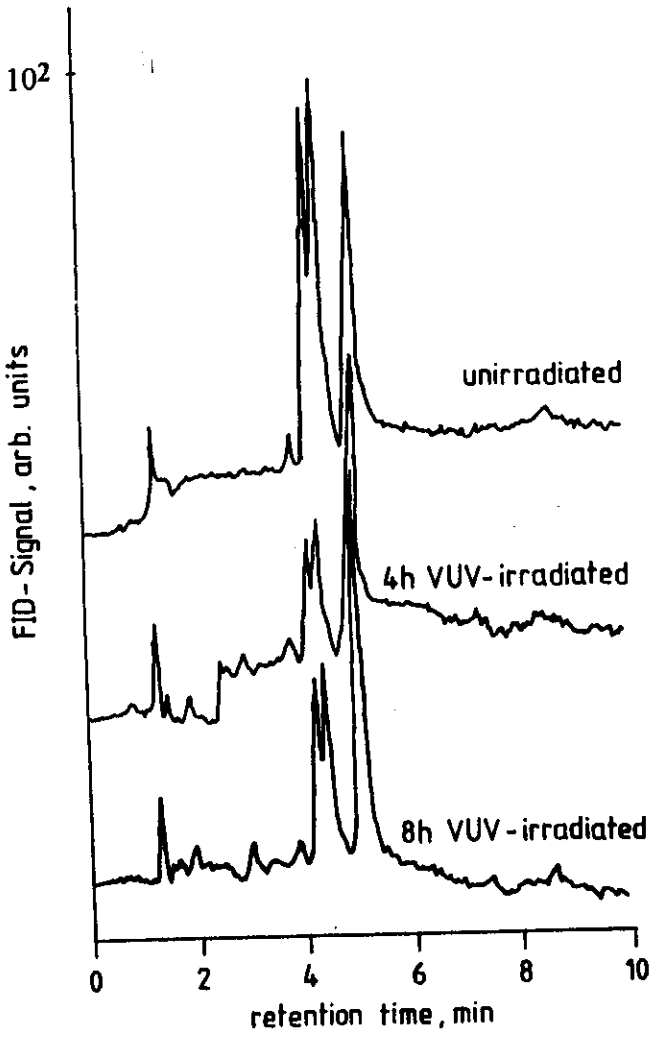

Fig. 40 : Comparison of GC chromatogram of tetracosane irradiated at 80 K for 4 h and 8 h with VUV photons with that of the unirradiated sample.

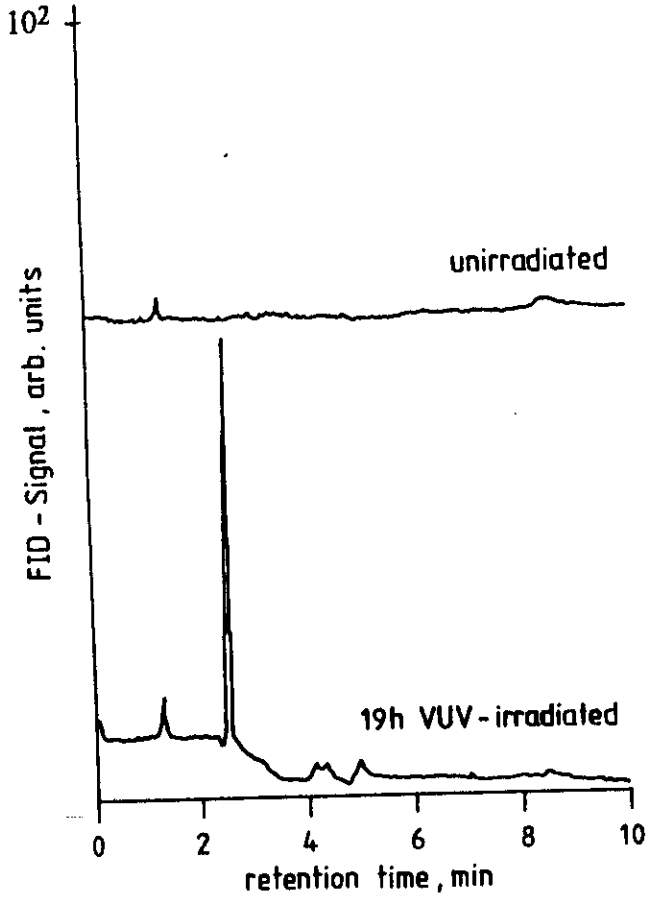

Fig. 41 : Comparison of GC chromatogram of androstane at 80 K irradiated for 8 h with that of VUV photons with the unirradiated sample.